

Alma Žiga<sup>1</sup>, Josip Kačmarčik<sup>2</sup>

# Plywood Cantilever Deflection: Experimental, Analytical and FEM Approach

## Progib konzole od furnirske ploče: eksperimentalni, analitički i FEM pristup

### ORIGINAL SCIENTIFIC PAPER

#### Izvorni znanstveni rad

Received – prispjelo: 13. 7. 2022.

Accepted – prihvaćeno: 4. 11. 2022.

UDK: 691.116

<https://doi.org/10.5552/drvind.2023.0053>

© 2023 by the author(s).

Licensee Faculty of Forestry and Wood Technology, University of Zagreb.

This article is an open access article distributed under the terms and conditions of the Creative Commons Attribution (CC BY) license.

**ABSTRACT** • *In this paper, the elastic behaviour in bending of three-layer plywood cantilever beams is analysed. Deflections of straight and half-circle cantilevers, loaded with a force at free end is determined experimentally and calculated using analytical and finite element method approach. The analytical calculation of deflection for the strait cantilever is obtained using a transformed cross section. The deflection of half-circle cantilever is determined by the classical laminated plate theory and Castigliano's theorem. Loads and cantilever dimensions are varied in the study using the design of experiment. The deflection regression models for straight and semi-circular plywood cantilevers are obtained from the experimental results. Analytically and numerically determined deflections of strait and half-circle cantilevers show very good agreement. Experimentally recorded deflections are approximately 30 % higher than analytical values. Stiffness properties and deflection values are influenced by direction of fibres in the outer layers of a three-layer plywood beam.*

**KEYWORDS:** *beam deflection; design of experiment; half-circle cantilever; orthotropic composite material; poplar plywood; straight cantilever*

**SAŽETAK** • *U radu je analizirano elastično ponašanje konzolnih greda od troslojne furnirske ploče pri savijanju. Progibi ravnih i polukružnih konzola opterećenih silom na slobodnom kraju određeni su eksperimentalno te izračunani analitičkim postupkom i metodom konačnih elemenata. Analitički proračun progiba ravne konzole dobiven je primjenom transformiranog presjeka. Progib polukružne konzole određen je klasičnom teorijom lamelirane ploče i Castiglianovim teoremom. Opterećenja i dimenzije konzola u istraživanju variraju u skladu s postavkom eksperimenta. Iz eksperimentalnih rezultata dobiveni su regresijski modeli progiba za ravne i polukružne konzole od furnirske ploče. Analitički i računski utvrđeni progibi ravnih i polukružnih konzola vrlo se dobro podudaraju. Eksperimentalno zabilježeni progibi približno su 30 % veći od analitički utvrđenih. Na svojstva krutosti i vrijednosti progiba grede od troslojne furnirske ploče utječe smjer vlakana u njezinim vanjskim slojevima.*

**KLJUČNE RIJEČI:** *progib grede; postavka eksperimenta; polukružna konzola; ortotropni kompozitni materijal; furnirska ploča od topolovine; ravna konzola*

<sup>1</sup> Author is Assoc. Prof. at University of Zenica, Mechanical Engineering Faculty, Zenica, Bosnia and Herzegovina. <https://orcid.org/0000-0002-1019-7543>

<sup>2</sup> Author is Assoc. Prof. at University of Zenica, Mechanical Engineering Faculty, Zenica, Bosnia and Herzegovina. <https://orcid.org/0000-0002-5219-2062>

## 1 INTRODUCTION

### 1. UVOD

Wood has anisotropic mechanical properties (Bodig and Jayne, 1993; Stark *et al.*, 2010), but when the principal axes coincide with the orientation of the grain, wood can be considered orthotropic and, in certain cases, transversely isotropic. Plywood is a wood-based laminate where wood material is adhesively bonded together. The macroscopic structure of plywood is created by gluing alternately arranged, thin cross-bands, i.e. veneers of various thickness. At microscopic level, a veneer is a lamina strengthened by cellulose fibres and surrounded by a matrix mainly composed of lignin. Analytical calculations of stiffness properties of plywood, as symmetric laminate, can be performed using the classical laminated plate theory (CLPT). A study (Merhar, 2020) had shown that the laminate theory, which was well established and applied in the world of synthetic composites, could also be applied to plywood composites. The influence of fibre reinforcement and wood species on the physical and mechanical properties of veneer plywood as well as on laminated veneer lumber was also investigated (Brezović *et al.*, 2003; Bal, 2014; Sikora *et al.*, 2019). The CLPT and the finite element method (FEM) were used in a study (Makowski, 2019) to determine stress distribution in individual layers of 18 mm thick beech plywood, in the 3-point flexural bending test. Analysis (Bal and Bektař, 2014) showed that the effects of tree species, direction of load, and type of adhesive on flexural properties were significant, and it was determined that the effect of the type of adhesive is based on the density of the plywood. The influence of the veneer composition on the mechanical properties of rectangular and curved form of laminated wood was investigated by FEM and transformed cross section method in (Hajdarević *et al.*, 2017). A research (Labans *et al.*, 2010) determined elastic properties for individual veneer specimens in order to evaluate the input data for plywood products analyses using FEM. The study (Merhar, 2021) emphasised the correct input for FEM. Veneer is usually produced by peeling, which exerts large bending deformations in the tangential direction, resulting in local cracks. Because of the small cracks, the tensile strength in the tangential direction is much lower (up to three-times lower) than the tensile strength of solid wood. When applying the laminate theory to plywood, the drawback could be the lack of input data as well as the variability of the data for particular tree species (the variability of wood properties in the main directions can be up to 10 %). A study (Wilczyński and Warmbier, 2012) determined the elastic moduli of veneers assembled in pine and beech plywood panels, where the effects of the resin type and the number of

veneer plies in the plywood were evaluated. It was concluded that glue line (with Young's modulus ranging from 1000 to 10 000 MPa) had negligible influence on Young's modulus of the veneer in the grain direction, while in perpendicular direction to the grain, Young's modulus of veneer had 19.4 % lower value for maximum glue modulus. It is pointed out that the properties of veneers assembled in plywood differed from those of the wood from which the veneers were made. In the research (Tsen, 2013), bending strength (*MOR*) and modulus of elasticity (*MOE*) of red seraya structural plywood were obtained by EN 310 three-point bending and EN 789 four-point bending test. Also *MOR* and *MOE* were obtained by FEM simulation. The FEM results were 39 % and 14 % higher than those from EN 310 and EN 789 experiments, respectively.

This study aims to investigate elastic properties and behaviour of plywood cantilever beams - straight and semicircle, and to provide and compare analytical, numerical and experimental calculation methods for the deflection at the free end, in the point where concentric force is applied. The motivation for the research was the problem of how to calculate deflection in the design of parts of toys and souvenirs made using CO<sub>2</sub> laser cutter from 4 mm plywood (Žiga *et al.*, 2018; Žiga and Begić-Hajdarević, 2021), which were subjected to bending. However, the calculation methods presented here could be implemented in the design of various plywood structures.

The analytical calculation of the deflection for straight cantilever was done using transformed cross section, but semicircle cantilever required CLPT approach and the use of Castigliano's theorem. As far as the authors were aware, the analytical calculation for deflection of semicircle, horizontally layered cantilever could not be found anywhere in the literature. The numerical calculations were done in FEM software, where cantilevers and boundary conditions were modelled and deflections at the free end were obtained. The deflections of plywood specimens were experimentally measured on coordinate measuring machine (CMM) and the results were used to obtain the power regression model. The design of the experiment was implemented to obtain the dimensions of cantilever beams and load values for the research. All the results were compared and analysed in the paper.

## 2 MATERIALS AND METHODS

### 2. MATERIJALI I METODE

#### 2.1 Plywood material and cantilever beam configurations

##### 2.1. Furnirska ploča i konfiguracija konzolnih greda

The deflection of straight (Figure 1a) and half-circle cantilevers (Figure 1b) from plywood is investi-

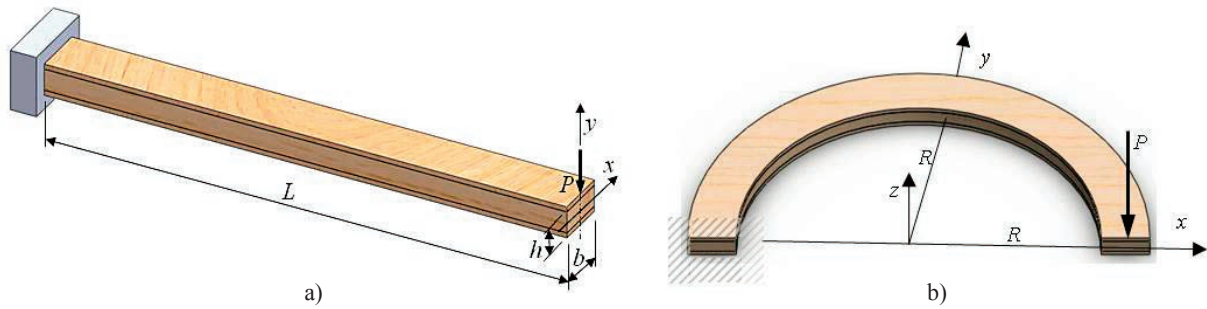


**Figure 1** Plywood cantilever beam configurations: a) straight, b) half-circle (P type)  
**Slika 1.** Konfiguracija konzolne grede od furnirske ploče: a) ravna, b) polukružna (tip P)

gated in the paper. The load at the end, the length of the straight or the radius of the half-circle cantilever and the cantilever width were varied, using the design of experiment.

Two types of poplar plywood sheets consisting of three veneer layers 4 mm thick were used: the first type with the central veneer 2.3 mm thick and the outside veneers 0.8 mm thick; and the second type, with three equal veneer thickness of 1.3 mm. Both sheets were acquired commercially, at a local store, with density of 410 kg/m<sup>3</sup> and with formaldehyde emission E1, measured in accordance with DIN EN 16516. This and similar types of plywood are often used for making toys and souvenirs, due to its characteristics such as low price and low density, which makes it easy to cut on small CO<sub>2</sub> laser cutter (80-120 kW power) and provides low weight of parts. Cantilever specimens from the first type of plywood, with central veneer thicker than outer ones, were cut so that the fibres in the outer layer were perpendicular to the cantilever span (label P, figure 1). Figure 2 shows plywood laser cut where a central veneer has fibres parallel to the cutting plane and outer veneer fibres are perpendicular to the cutting plane. Cantilever specimens from the second type of plywood, with the equal veneer thickness, were cut so that the outer layer fibres were longitudinal to the span of cantilever (label L).

Poplar veneers are orthotropic material with nine independent constants of material. In the analytical calculation and FEM analysis, the properties for poplar

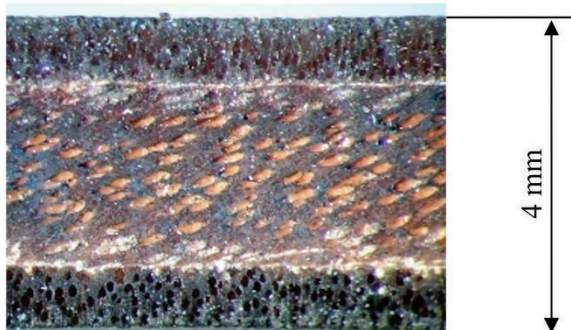


**Figure 2** Laser-cut of poplar plywood, 4 mm in thickness  
**Slika 2.** Laserski izrezana furnirska ploča od topolovine debljine 4 mm

veneer were taken from the paper (Brezović, *et al.*, 2003):  $E_1 = 9600$  MPa,  $E_2 = 420$  MPa,  $E_3 = 880$  MPa,  $\nu_{12} = 0.39$ ,  $\nu_{23} = 0.33$ ,  $\nu_{13} = 0.32$ ,  $G_{12} = 660$  MPa,  $G_{13} = 720$  MPa,  $G_{23} = 110$  MPa. Glue layer thickness can be observed in Fig. 2. It is a white layer, partially absorbed by adjacent wood layers. In numerical and analytical model, the average value of thickness was set to be 0.05 mm. As there were no data about glue line modulus, it was assumed that the value of this modulus for formaldehyde-based adhesives could range from 1000 to 10000 MPa (Wilczyński and Warmbier, 2012). The lowest value of 1000 MPa was chosen. Poisson ratio was set to 0.2 (Piao *et al.*, 2008).

**2.2 Design of experiment**  
**2.2. Postavke eksperimenta**

Full orthogonal, three-factor plan (Figure 3), with 4 measurement repetitions in central plan point is implemented in the paper thus making  $N = 2^k + n_0 = 2^3 + 4 = 12$  experimental runs. The 12 experimental runs are required for each of the two types of plywood fibre orientation and for two different geometries of cantilever beam, making it in total 48 experimental runs. The model factors for experiment are:  $x_1$  – load ( $P$ ),  $x_2$  - length for straight cantilever ( $L$ ) or radius for half-circle cantilever ( $R$ ) and  $x_3$  - width of cross-section

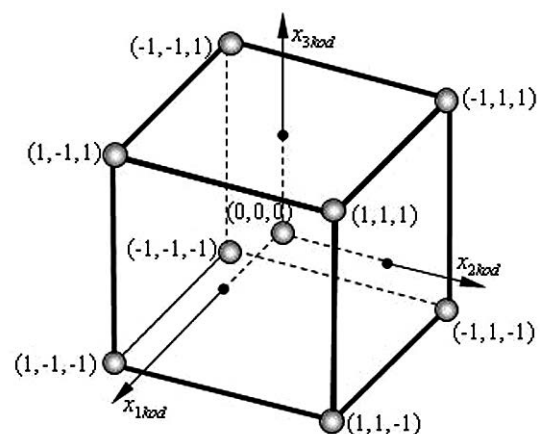


**Figure 3** Location of experimental points of full orthogonal plan in hyper-space  
**Slika 3.** Položaj eksperimentalnih točaka cijele ortogonalne projekcije u hiperprostoru

**Table 1** Experiment design matrix  
**Tablica 1.** Matrica postavki eksperimenta

Exp. runs	1	2	3	4	5	6	7	8	9	10	11	12
$x_1 (P)$	-1	1	-1	1	-1	1	-1	1	0	0	0	0
$x_2 (L \text{ or } R)$	-1	-1	1	1	-1	-1	1	1	0	0	0	0
$x_3 (b)$	-1	-1	-1	-1	1	1	1	1	0	0	0	0

(b), see Figure 3. The experiment design matrix, for both investigated cantilevers, is presented in Table 1.

Levels of loads and dimensions are arbitrarily chosen to produce measurable deflection but also not to exert stresses above material strength. The cantilever dimensions also correspond to the dimensions of possible parts in mechanical toys and souvenirs (Žiga *et al.*, 2018). The level values for straight and half-circle cantilever of all factors are shown in Table 2. The basic level was chosen to be geometrical mean of the upper and lower level.

It can be observed from the experiment design matrix that five different specimen dimension configurations are needed. The five test specimens were laser-cut for each of the two types of plywood fibre orientation. Figure 4 shows straight and half circle cantilever specimens with fibres in outer ply perpendicular to the span (P-type). On one side of the specimens, there is a wide segment for clamping, and on the other a segment with the narrow lateral groove for positioning the load.

From the experimental results, power regression models that provide a relation between three independent variables ( $x_1, x_2, x_3$ ) and the deflection as a dependent variable is determined. The power regression model for straight cantilevers is obtained using last squared method. The paper by Žiga *et al.* (2019) presents in detail how to determine coefficients of power model function.

**2.3 Analytical method for cantilever deflection**

**2.3. Analitička metoda za izračun otklona konzole**

**2.3.1 Deflection of straight cantilever**

**2.3.1. Otklon ravne konzole**

The straight cantilever loaded with concentrated force at the end of the span (Figure 1a) is analysed. In the cross-section, the cantilever is a symmetrical composite laminate made of veneer sheets and adhesive layers, so the method of transformed cross section can be applied (Bodig and Jayne, 1993). In this method,

**Table 2** Levels of model factors  
**Tablica 2.** Razine faktora modela

Factor / Faktor		Straight cantilever / Ravna konzola			Half-circle cantilever / Polukružna konzola		
		Low level Niža vrijednost	Basic level Srednja vrijednost	High level Viša vrijednost	Low level Niža vrijednost	Basic level Srednja vrijednost	High level Viša vrijednost
Load / opterećenje (P)	N	0.5	0.736	1.01	0.5	0.736	1.01
	$x_1$	-1	0	+1	-1	0	+1
Length (L) or Radius (R) duljina (L) ili radijus (R)	mm	80	100	120	26	34	42
	$x_2$	-1	0	+1	-1	0	+1
Width / širina (b)	mm	6	8	10	7	8	9
	$x_3$	-1	0	+1	-1	0	+1



**Figure 4** P-type specimens: a) straight cantilever, b) half-circle cantilever  
**Slika 4.** Uzorci tipa P: a) ravna konzola, b) polukružna konzola

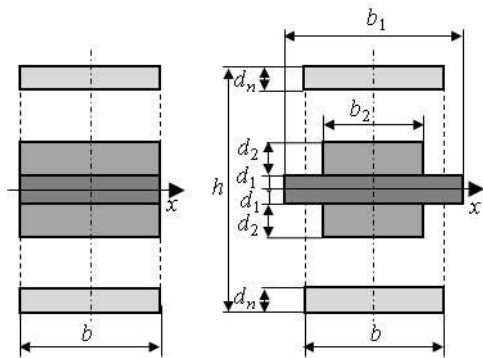


**Figure 5** Plywood cross section: a) original, b) transformed  
**Slika 5.** Presjek furnirske ploče: a) izvorni, b) transformirani

only one reference value of the elasticity modulus e.g. the outer lamina elasticity modulus  $E_n$ , in the direction of the cantilever span, is used in the deflection calculation. The transformed cross-section (Figure 5) is made so that lamina other than the reference one has a transformed width defined by

$$b_i = b \left( \frac{E_i}{E_n} \right) \quad (1)$$

Where  $b$  is the original width of the lamina,  $E_i$  is the lamina modulus of elasticity in the direction of span,  $E_n$  is the modulus of elasticity of the reference lamina. Thicknesses of all lamina do not change; the original values are used. The moment of inertia  $I_x$  of the transformed cross section with  $n$  lamina in one symmetrical half of the cross section (Figure 5) is calculated with:

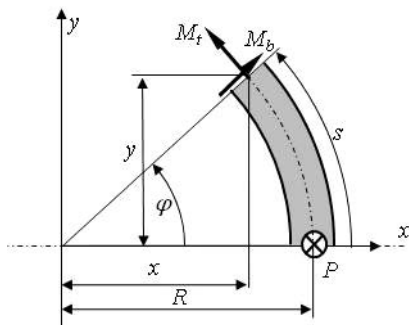
$$I_x = \frac{2 \cdot b}{E_n} \sum_{i=1}^n \left[ \frac{E_i \cdot d_i^3}{12} + E_i \cdot d_i \left( \sum_{j=1}^{i-1} d_j + \frac{d_i}{2} \right)^2 \right] \quad (2)$$

Where  $d_i$  is the thickness of the  $i$ -lamina.

After the transformed cross section is defined, the deflection of the cantilever is calculated with:

$$\delta = \frac{P \cdot L^3}{3 \cdot E_n \cdot I_x} \quad (3)$$

Where  $P$  is the load at the end of cantilever and  $L$  is the length of cantilever.



### 2.3.2 Deflection of half-circle cantilever

#### 2.3.2. Otklon polukružne konzole

The deflection of the half-circle cantilever (Figure 1b) at the point of application of the force  $P$  and in the direction of the force will be determined using procedures from Horibe and Mori, 2015; Dahlberg, 2004 and Žiga *et al.*, 2018.

Figure 6a shows cross-section of the beam situated at angle  $\varphi$ . The force  $P$  is normal to the  $xy$  plane. The bending moment  $M_b$  and torsional moment  $M_t$  are acting on this cross-section. The shear force is omitted in the figure since its influence on beam deflection can be neglected. For positive values of  $x$  and  $y$ , angle  $\varphi$  varies between 0 and  $\pi/2$ , so both  $\cos\varphi$  and  $\sin\varphi$  have positive values. From the moment equilibrium equations about  $x$  and  $y$  axes, the moments  $M_b$  and  $M_t$  are:

$$M_b = -P [y \cos \varphi + (R - x) \sin \varphi] = -P \cdot R \sin \varphi \quad (4)$$

$$M_t = P [(-R + x) \cos \varphi + y \sin \varphi] = P \cdot R (1 - \cos \varphi) \quad (5)$$

The strain-stress relation for unidirectional laminate (Figure 6b) in its plane (Jones, 1999; Cuntze, 2015) is:

$$\begin{Bmatrix} \epsilon_x \\ \epsilon_y \\ \gamma_s \end{Bmatrix} = \begin{bmatrix} S_{xx} & S_{xy} & S_{xs} \\ S_{yx} & S_{yy} & S_{ys} \\ S_{sx} & S_{sy} & S_{ss} \end{bmatrix} \cdot \begin{Bmatrix} \sigma_x \\ \sigma_y \\ \tau_s \end{Bmatrix} \quad (6)$$

Where  $S_{ij}$  are the transformed compliance coefficients for in-plane behaviour;  $\epsilon_x, \epsilon_y$  are the in-plane normal strains;  $\gamma_s$  is the in-plane shear strain;  $\sigma_x, \sigma_y$  are the in-plane normal stresses;  $\tau_s$  is the in-plane shear stress. The  $xyz$  coordinate system in Figure 6b is assumed to have its origin in the middle of the laminate thickness.

Applying classical laminated plates theory, the following relationships can be obtained (Daniel *et al.*, 2006):

$$\begin{Bmatrix} \kappa_x \\ \kappa_y \\ \kappa_s \end{Bmatrix} = \frac{12}{h^3} \begin{bmatrix} S_{xx} & S_{xy} & S_{xs} \\ S_{yx} & S_{yy} & S_{ys} \\ S_{sx} & S_{sy} & S_{ss} \end{bmatrix} \cdot \begin{Bmatrix} m_x \\ m_y \\ m_s \end{Bmatrix} \quad (7)$$

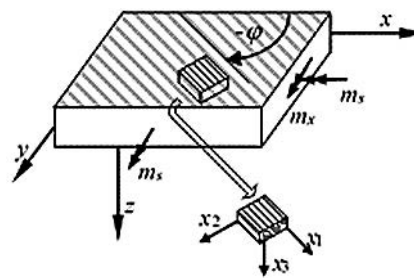


**Figure 6** a) Moment equilibrium b) Moments acting on composite cantilever segment  
**Slika 6.** a) Momenti ravnoteže, b) momenti koji djeluju na segment kompozitne konzole

$$\begin{Bmatrix} \sigma_x \\ \sigma_y \\ \tau_s \end{Bmatrix} = z \cdot \frac{12}{h^3} \begin{Bmatrix} m_x \\ m_y \\ m_s \end{Bmatrix} \quad (8)$$

Where  $m_x, m_y$  are the bending moments per unit length;  $m_s$  is the twisting moment per unit length;  $\kappa_x, \kappa_y$  are the bending curvatures of the middle surface;  $\kappa_s$  is the twisting curvature of the middle surface.

Strain energy per unit volume for linearly elastic behaviour induced by bending and twisting is (Mujika and Mondragon, 2003):

$$u_M = \frac{1}{2} (\sigma_x \cdot \epsilon_x + \sigma_y \cdot \epsilon_y + \tau_s \cdot \gamma_s) \quad (9)$$

Substituting stress-strain relations from Equation (6):

$$u_M = \frac{1}{2} (S_{xx} \sigma_x^2 + S_{yy} \sigma_y^2 + S_{ss} \tau_s^2) + S_{xy} \sigma_x \sigma_y + S_{xs} \sigma_x \tau_s + S_{ys} \sigma_y \tau_s \quad (10)$$

Elastic strain energy stored in the beam is:

$$U = \int_V u_M dV \quad (11)$$

Considering 3 plies of veneer and 2 plies of glue line, angle  $\varphi$  of fibre direction, bending and torsional moments as:

$$m_x = \frac{M_b}{b}, m_y = 0, m_s = -\frac{M_t}{2b} \quad (12)$$

The strained energy is:

$$U = \left(\frac{12}{h^3}\right)^2 \cdot \left( \frac{1}{2} \int_V \left(\frac{M_b}{b}\right)^2 b R d\varphi \cdot S_{xx} z^2 dz + \frac{1}{2} \int_V \left(-\frac{M_t}{2b}\right)^2 b R d\varphi \cdot S_{ss} z^2 dz - \int_V \frac{M_b}{b} \frac{M_t}{2b} b R d\varphi \cdot S_{xs} z^2 dz \right) \quad (13)$$

Where

$$\int_0^h S_{ij} z^2 dz = d_{ij} = \frac{1}{3} \sum_{k=1}^5 S_{ij}^k (z_k^3 - z_{k-1}^3) \quad (14)$$

Transformed compliance coefficients are expressed with compliance coefficients in fiber direction coordinate system:

$$\begin{aligned} c &= \cos \varphi, s = \sin \varphi \\ S_{xx} &= c^4 S_{11} + s^4 S_{22} + (2S_{12} + S_{66}) c^2 s^2 \\ S_{xs} &= (2S_{11} - 2S_{12} - S_{66}) c^3 s - (2S_{22} - 2S_{12} - S_{66}) c s^3 \\ S_{ss} &= (4S_{11} + 4S_{22} - 8S_{12}) c^2 s^2 + (c^2 - s^2) S_{66} \end{aligned} \quad (15)$$

Compliance coefficients in fiber direction or principal material coordinate system (Figure 6b) are:

$$S_{11} = \frac{1}{E_1}, S_{22} = \frac{1}{E_2}, S_{66} = \frac{1}{G_{12}}, S_{12} = S_{21} = -\frac{V_{12}}{E_1} = -\frac{V_{21}}{E_2} \quad (16)$$

Using Castigliano's theorem, the deflection of the cantilever end, at the load  $P$  can be calculated with:

$$\delta = \frac{\partial U}{\partial P} = \left(\frac{12}{h^3}\right)^2 \cdot \left( \begin{aligned} &\frac{1}{b} \int_0^\pi M_b \frac{\partial M_b}{\partial P} d_{xx} R d\varphi + \\ &+ \frac{1}{4b} \int_0^\pi M_t \frac{\partial M_t}{\partial P} d_{ss} R d\varphi - \\ &- \frac{1}{2b} \int_0^\pi \left(\frac{\partial M_b}{\partial P} M_t + M_b \frac{\partial M_t}{\partial P}\right) d_{xs} R d\varphi \end{aligned} \right) \quad (17)$$

## 2.4 Cantilever deflection using FEM

### 2.4. Otklon konzole dobiven metodom konačnih elemenata

Numerical analysis is performed using commercial software SolidWorks 2020 and its Simulation module based on the finite element method (FEM). Five FE models of straight beam cantilever and five models of half-circle beam cantilever were modelled with dimensions that are defined by design of experiment (Tables 1 and 2) and to be geometrically identical to the real specimens. Models were positioned in Cartesian co-ordinate system where the directions of co-ordinates coincide with three main directions of material axes. Composite material was defined in software using material properties from literature (see chapter 2.1)

The boundary conditions in FEM analysis were defined to correspond as much as possible to the actual experimental conditions. Thus, the results achieved by numerical method could be compared to the experiment results. The left segment for clamping was fixed and force was applied on the line between lateral grooves on the right segment for load. The automatic meshing from Solidworks was used with the fine mesh quality setting in order to obtain accurate results. Figure 7a shows an example of FEM model of straight cantilever with P-type fibre orientation (length 80 mm and

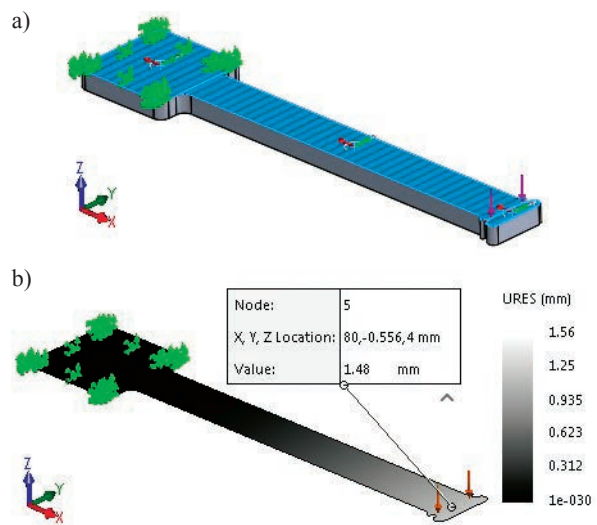


**Figure 7** Straight cantilever FEM ( $L = 80$  mm,  $b = 10$  mm,  $P = 1.01$  N), P-type: a) boundary condition, b) deflection result  
**Slika 7.** Ravna konzola FEM ( $L = 80$  mm,  $b = 10$  mm,  $P = 1,01$  N), tip P: a) rubni uvjet, b) otklon

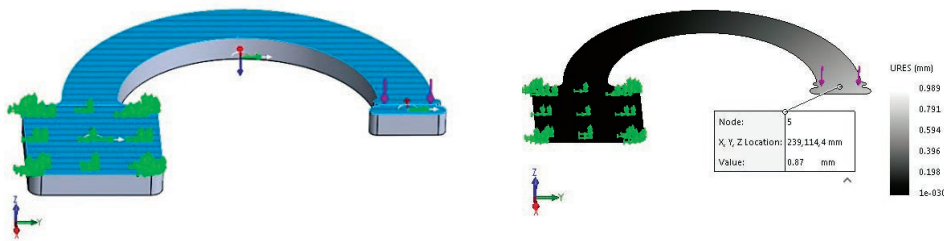
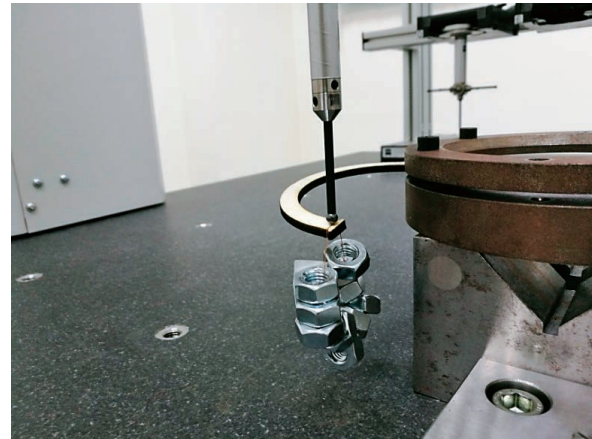


**Figure 8** Half-circle cantilever FEM ( $R = 26$  mm,  $b = 9$  mm,  $P = 1.01$  N), P-type: a) boundary condition, b) deflection result  
**Slika 8.** Polukružna konzola FEM ( $R = 26$  mm,  $b = 9$  mm,  $P = 1,01$  N), tip P: a) rubni uvjet, b) otklon



a)



b)

**Figure 9** a) CMM „ZEISS CONTURA G2”, b) Measurement of deflection on CMM  
**Slika 9.** a) CMM „ZEISS CONTURA G2”; b) mjerenje otklona na CMM-u

width 10 mm). Figure 8a shows an example of FEM model of half-circle cantilever with P-type fibre orientation (radius 26 mm and width 9 mm). Figure 7b and Figure 8b show deflection results after finished FEM simulations for the above-mentioned examples.

## 2.5 Experimental study

### 2.5. Eksperimentalno istraživanje

CMM “ZEISS CONTURA G2” was used (Figure 9a) for the experimental measurements of plywood cantilever deflections. The CMM was equipped with the continuous scanning probe system “VAST XT”. The measuring uncertainty of the CMM is 1.8  $\mu$ m, which makes it a very accurate measuring device. For the measurement of the deflections, the cantilevers specimens were positioned and clamped on the CMM table. The specimens were fixed between two steel parts fastened with bolts. The parts were fixed on the CMM table with magnetic V-block (Figure 9b). At the free end of the specimens, the load was applied by hanging an appropriate weight made from steel nuts (Figure 9b). The deflection of the cantilever was measured as a difference between vertical coordinate reading of the CMM before and after loading. The CMM probing of the cantilever end point where load was applied, before and after loading, was done manually.

## 3 RESULTS AND DISCUSSION

### 3. REZULTATI I RASPRAVA

#### 3.1 Results for straight cantilever

##### 3.1. Rezultati za ravnu konzolu

For straight cantilevers, analytical, numerical, experimental and regression model results values, for the end-point deflections for the P-type and L-type fiber orientation, respectively, are presented in Table 3 and 4. The last row shows deviation in results between experimental and analytical values. Figures 10a and 10b show the above mentioned deflection values on charts.

Analytical and numerical deflection values are very close to each other. Differences are visible only in the second decimal place. These values are, on average, 30 % lower than deflection recorded by the experiment. The differences are lower for the greater cantilever length due to slope contribution to a deflection value.

For P-type straight cantilever, the regression model is:

$$\delta_p = 0.009857 \cdot P^{1.04} \cdot L^{1.8486} \cdot b^{-1.0629} \quad (18)$$

The regression model for L-type straight cantilever is:

$$\delta_L = 0.003132 \cdot P^{1.0787} \cdot L^{1.7658} \cdot b^{-0.9977} \quad (19)$$

For the evaluation of the models, statistical data analysis has been used. Some results are presented in Table 5. The coefficient of determination ( $R^2$ ), adjusted

**Table 3** Results for P-type straight cantilever beam  
**Tablica 3.** Rezultati ispitivanja ravne konzolne grede tipa P

Exp. run	1	2	3	4	5	6	7	8	9	10	11	12
$y_{exp}$ , mm	2.40	4.77	5.22	10.72	1.31	3.23	3.06	5.78	3.88	3.79	3.55	3.74
$y_{mod}$ , mm	2.36	4.88	5.15	10.62	1.31	2.71	2.86	5.90	3.88	3.88	3.88	3.88
$y_{an}$ , mm	1.22	2.47	4.13	8.34	0.73	1.48	2.48	5.00	2.64	2.64	2.64	2.64
$y_{num}$ , mm	1.22	2.44	4.10	8.28	0.73	1.48	2.46	4.98	2.61	2.61	2.61	2.61
$\frac{y_{exp} - y_{an}}{y_{exp}}$ , %	49.0	48.2	20.9	22.2	44.0	54.1	19.0	13.4	32.0	30.4	25.7	29.5

**Table 4** Results for L-type straight cantilever beam  
**Tablica 4.** Rezultati ispitivanja ravne konzolne grede tipa L

Exp. run	1	2	3	4	5	6	7	8	9	10	11	12
$y_{exp}$ , mm	0.47	1.32	1.08	2.53	0.42	0.56	0.62	1.45	0.99	1.21	0.95	1.10
$y_{mod}$ , mm	0.57	1.22	1.17	2.49	0.34	0.73	0.70	1.49	0.96	0.96	0.96	0.96
$y_{an}$ , mm	0.29	0.59	0.98	1.97	0.17	0.35	0.59	1.18	0.62	0.62	0.62	0.62
$y_{num}$ , mm	0.29	0.59	0.98	1.98	0.17	0.35	0.59	1.19	0.63	0.63	0.63	0.63
$\frac{y_{exp} - y_{an}}{y_{exp}}$ , %	38.6	55.5	9.8	21.9	58.8	36.9	5.5	18.1	36.9	48.6	34.3	43.3

$R^2$ , standard error, regression sum of squares and the result of  $F$ -test were used for checking the adequacy of the model. The value of  $R^2$  for the P-type of cantilever, where fibres in outer plies are perpendicular to the length, is quite high ( $R^2 = 0.98$ ). It means that 98 % of cantilever deflection variability was caused by the variation of load  $P$ , length  $L$  and width  $b$  of the cantilever. Only 2 % of the variability was caused by some other factors, which were not included in the experiment (factors that were not controlled). For L-type of cantilever, 12 % of variability was caused by some other factors. It was explained by lower range of deflection

(0.42 to 1.44 mm) in comparison to the first type of cantilever (deflection range is: 1.31 - 10.72 as shown in Figure 10a).

**3.1 Results for half-circle cantilever**  
**3.1. Rezultati za polukružnu konzolu**

For half-circle cantilevers, analytical, numerical, experimental and regression model results values, for the end point deflections, are presented in Table 6. The last columns for each type of cantilever show differences between experimental and analytical values. The differences between analytical and numerical results

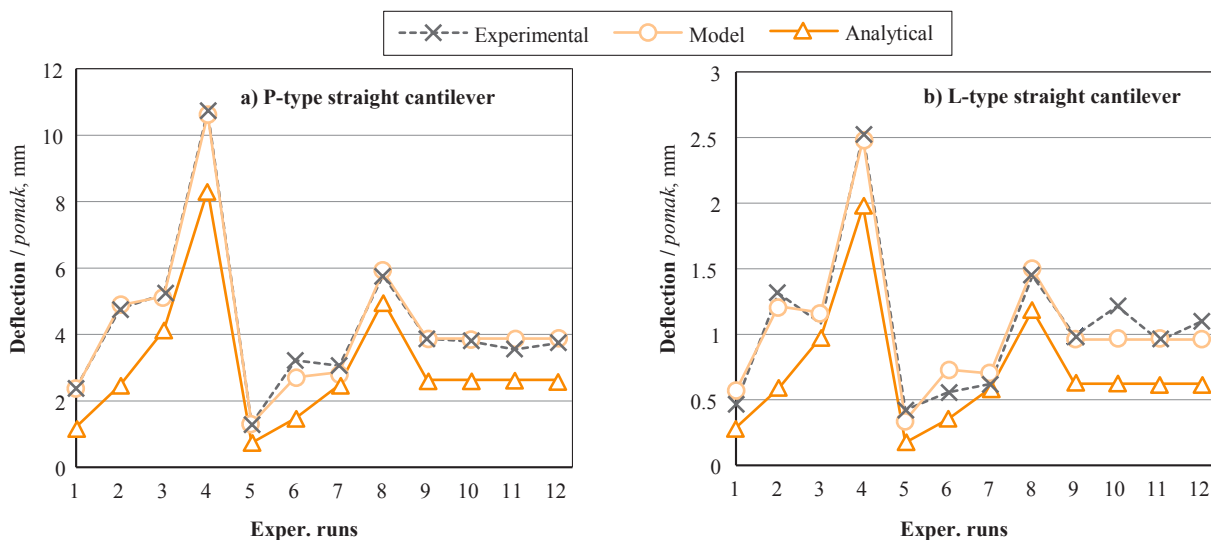


**Figure 10** Experimental results, regression model and analytical results for deflection of: a) P-type straight cantilever, b) L-type straight cantilever

**Slika 10.** Eksperimentalni rezultati, regresijski model i analitički rezultati odklona: a) ravne konzole tipa P, b) ravne konzole tipa L

**Table 5** Data analysis for regression model of straight cantilever  
**Tablica 5.** Analiza podataka za regresijski model ravne konzole

Data / Podatak	P-type	L-type
$R^2$	0.9859	0.9137
Adjusted $R^2$ / prilagođeni $R^2$	0.9807	0.8814
Standard error / standardna pogreška	0.0705	0.1785
Regression sum of squares / regresijski zbroj kvadrata	2.7893	2.6998
$F_{value}$	186.8291	28.2423
$F_{table}$	$F_0(3;8;0.05)=4.07$	$F_0(3;8;0.05)=4.07$
Model is adequate odgovarajući model	Yes ( $F_0 < F$ )	Yes ( $F_0 < F$ )

are greater than for the straight cantilever, but still the results are very close. The greater differences could be explained by more complex analytical approach. Figure 11 shows graphical representation of deflection values for different methods for P and L type of cantilevers, respectively.

Power regression model for P-type, half-circle cantilever is:

$$\delta_p = 0.002107 \cdot P^{1.164} \cdot R^{3.3123} \cdot b^{-1.9705} \quad (20)$$

and for the L-type, half-circle cantilever is:

$$\delta_L = 0.00313 \cdot P^{1.0787} \cdot R^{1.766} \cdot b^{-0.9977} \quad (21)$$

Statistical data analysis is shown in Table 8. Values of  $R^2$  for both types of cantilevers are quite high. Analytical values are, on average, 24 % lower than deflection recorded by the experiment for P-type of half-circle cantilever and 25 % for L-type.

#### 4 CONCLUSIONS 4. ZAKLJUČAK

Analytically and numerically determined deflections of straight and half-circle cantilever showed very good agreement. Experimentally recorded deflections

**Table 6** Results for P-type straight cantilever beam  
**Tablica 6.** Rezultati ispitivanja polukružne konzolne grede tipa P

Exp. run	1	2	3	4	5	6	7	8	9	10	11	12
$y_{exp}$ , mm	0.80	1.88	5.24	10.68	0.61	1.45	2.41	5.21	3.53	3.66	3.34	3.32
$y_{mod}$ , mm	0.99	2.24	4.84	10.97	0.60	1.37	2.95	6.68	2.90	2.90	2.90	2.90
$y_{an}$ , mm	0.75	1.52	3.18	6.41	0.59	1.18	2.47	4.99	2.17	2.17	2.17	2.17
$y_{num}$ , mm	0.72	1.45	3.14	6.34	0.46	0.93	1.93	3.90	1.76	1.76	1.76	1.76
$\frac{y_{exp} - y_{an}}{y_{exp}}$ , %	5.8	19.1	39.4	39.9	4.0	18.4	2.5	4.2	38.5	40.7	35.0	34.7

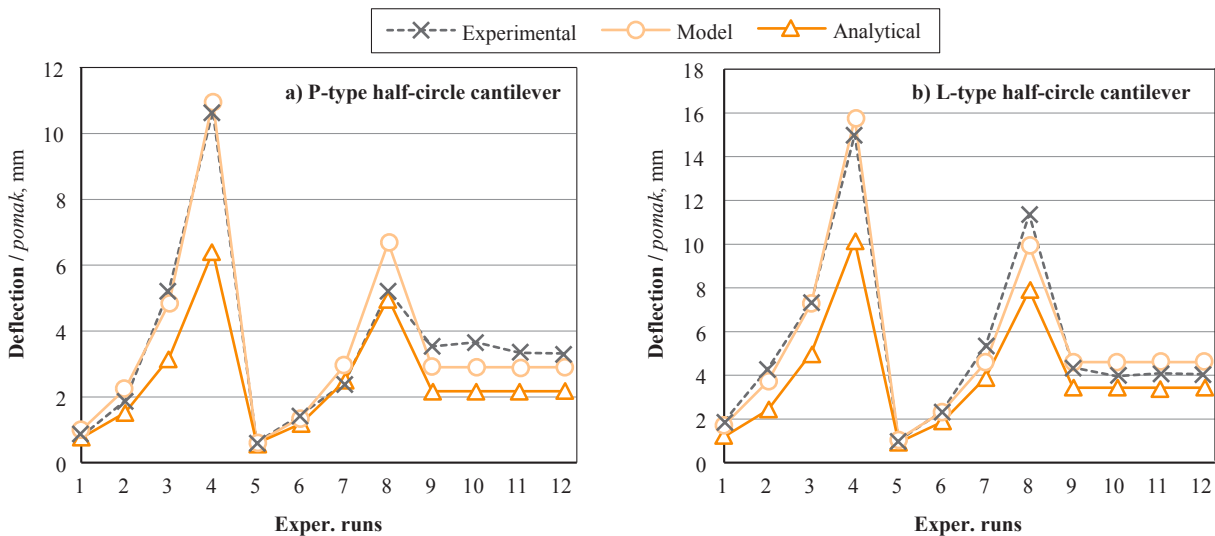


**Figure 11** Experimental results, regression model and analytical results for deflection of: a) P-type half-circle cantilever, b) L-type half-circle cantilever  
**Slika 11.** Eksperimentalni rezultati, regresijski model i analitički rezultati otklona: a) polukružne konzole tipa P, b) polukružne konzole tipa L

**Table 7** Results for L-type straight cantilever beam**Tablica 7.** Rezultati ispitivanja polukružne konzolne grede tipa L

Exp. run	1	2	3	4	5	6	7	8	9	10	11	12
$y_{exp}$ , mm	1.90	4.30	7.33	15.01	1.01	2.36	5.36	11.36	4.36	3.96	4.09	4.05
$y_{mod}$ , mm	1.71	3.71	7.28	15.76	1.08	2.33	4.58	9.92	4.60	4.60	4.60	4.60
$y_{an}$ , mm	1.19	2.41	5.02	10.14	0.93	1.87	3.90	7.89	3.43	3.43	3.43	3.43
$y_{num}$ , mm	1.20	2.43	5.14	10.37	0.84	1.71	3.60	7.29	3.29	3.29	3.29	3.29
$\frac{y_{exp} - y_{an}}{y_{exp}}$ , %	37.3	44.1	31.5	32.5	8.3	20.7	27.2	30.6	21.3	13.4	16.1	15.3

**Table 8** Data analysis for regression model of half-circle cantilever**Tablica 8.** Analiza podataka za regresijski model polukružne konzole

Data / Podatak	P-type	L-type
$R^2$	0.956	0.977
Adjusted $R^2$ / prilagođeni $R^2$	0.939	0.968
Standard error / standardna pogreška	0.201	0.131
Regression sum of squares / regresijski zbroj kvadrata	6.915	5.839
$F_{value}$	57.327	28.2423
$F_{table}$	F0(3;8;0.05)=4.07	F0(3;8;0.05)=4.07
Model is adequate / odgovarajući model	Yes (F0<F)	Yes (F0<F)

were approximately 30 % higher than analytical values. The weakness of the analytical and numerical approach lied in the lack of knowledge of the input data for the wood tissue. The mean values were taken from the publicly available literature (Brezović *et al.*, 2003). Another weakness was the presentation of glue line and lack of its properties. Glue line was modelled with a uniform thickness and with the smallest modulus of elasticity.

This study showed that CLPT and Castigliano's theorem could be used to analytically obtain deflection of half-circle, multi-layer composite structure and this approach had never been presented in the publicly available literature as far as the authors were aware.

For straight, three-layer plywood cantilevers, direction of fibres in outer layers has great influence on stiffness properties and deflection values. When fibres in outer layers were perpendicular to the cantilever span (P type), the stiffness was lower and deflection was higher. Experimental deflection values for P type cantilevers were 1.31 to 10.72 mm. For L type cantilevers, the deflections were 0.42 to 1.44 mm.

For half-circle, three-layer plywood cantilevers, direction of fibres in outer layers has medium influence on stiffness properties and deflection values. When fibres in outer layers were perpendicular to the cantilever span, experimentally recorded values were 0.61 to 10.68 mm (P type). For L type, experimentally recorded values were 1.01 to 15.01 mm.

The implementation of design of experiment is proved as an efficient way to obtain regression model for the deflection of plywood beam. Model predicted values are very close to the experimentally obtained values. In

the observed experiments, the length of straight cantilever ( $L$ ) or the radius of half-circle cantilever ( $R$ ) has the most influence on the beam deflection, more than the force ( $P$ ) and width of the beam ( $b$ ). The  $L$  or  $R$  have the standardized coefficient with the largest absolute value and this means that  $L$  or  $R$  are the most important independent variable in the regression model.

## 5 REFERENCES

### 5. LITERATURA

- Bal, B. C., 2014: Some physical and mechanical properties of reinforced laminated veneer lumber. *Construction and Building Materials*, 68: 120-126. <https://doi.org/10.1016/j.conbuildmat.2014.06.042>
- Bal, B. C.; Bektař, Ů., 2014: Some mechanical properties of plywood produced from eucalyptus, beech and poplar veneer. *Maderas, Ciencia y tecnología*, 16 (1): 99-108. <https://doi.org/10.4067/s0718-221x2014005000009>
- Bodig, J.; Jayne, B. A., 1993: *Mechanics of wood and wood composites*. Melbourne: Krieger Publishing Company.
- Brezović, M.; Jambrekić, V.; Pervan, S., 2003: Bending properties of carbon fibre reinforced plywood. *Wood Research*, 48 (4): 13-24.
- Cuntze, R., 2015: Classical Laminate Theory (CLT) for laminates composed of unidirectional (UD) laminae, analysis flow chart, and related topics (online). [https://www.researchgate.net/publication/314472082\\_HANDBUCH\\_STRUKTUR\\_BERECHNUNG\\_HSB\\_Overlay\\_WS-YHSB001uk\\_Classical\\_Laminate\\_Theory\\_CLT\\_for\\_laminates\\_composed\\_of\\_unidirectional\\_UD\\_laminae\\_analysis\\_flow\\_chart\\_and\\_related\\_topics\\_\(Accessed\\_May\\_18\\_2022\)](https://www.researchgate.net/publication/314472082_HANDBUCH_STRUKTUR_BERECHNUNG_HSB_Overlay_WS-YHSB001uk_Classical_Laminate_Theory_CLT_for_laminates_composed_of_unidirectional_UD_laminae_analysis_flow_chart_and_related_topics_(Accessed_May_18_2022)).
- Dahlberg, T., 2004: Procedure to calculate deflections of curved beams. *International Journal of Engineering Education*, 20 (3): 503-513.

7. Daniel, I. M.; Ishai, O.; Daniel, I., 2006: Engineering mechanics of composite materials. Oxford University Press, New York.
8. Hajdarevic, S.; Obucina, M.; Mesic, E., 2017: Effect of veneer composition on the stiffness and stress of laminated wood. Vienna, Annals of DAAAM & Proceedings, pp. 28.
9. Horibe, T.; Mori, K., 2015: In-plane and out-of-plane deflection of J-shaped beam. *Journal of Mechanical Engineering and Automation*, 5(1), pp. 14-19. <https://doi.org/10.5923/j.jmea.20150501.02>
10. Jones, R. M., 1999: *Mechanics of Composite Materials*. Taylor & Francis Group, New York.
11. Labans, E.; Kalninsh, K.; Ozolinsh, O., 2010: Experimental and numerical identification of veneers mechanical properties. *Scientific Journal of Riga Technical University*, 11: 38-43.
12. Makowski, A., 2019: Analytical analysis of distribution of bending stresses in layers of plywood with numerical verification. *Drvna industrija*, 70 (1): 77-88. <https://doi.org/10.5552/drwind.2019.1823>
13. Merhar, M., 2020: Determination of elastic properties of beech plywood by analytical, experimental and numerical methods. *Forests*, 11 (11): 1221. <https://doi.org/10.3390/f11111221>
14. Merhar, M., 2021: Application of failure criteria on plywood under bending. *Polymers*, 13 (24): 4449. <https://doi.org/10.3390/polym13244449>
15. Mujika, F.; Mondragon, I., 2003: On the displacement field for unidirectional off-axis composites in 3-point flexure. Part I: Analytical approach. *Journal of Composite Materials*, 37 (12): 1041-1066. <https://doi.org/10.1177/0021998303037012001>
16. Piao, C.; Shupe, T. F.; Tang, R. C.; Hse, C. Y., 2008: Finite element modeling of small-scale tapered wood-laminated composite poles with biomimicry features. *Wood and Fibre Science*, 40 (1): 3-13.
17. Sikora, A.; Svoboda, T.; Záborský, V.; Gaffová, Z., 2019: Effect of selected factors on the bending deflection at the limit of proportionality and at the modulus of rupture in laminated veneer lumber. *Forests*, 10 (5): 401. <https://doi.org/10.3390/f10050401>
18. Stark, N. M.; Cai, Z.; Carll, C. G., 2010: *Wood handbook*, Chapter 11: Wood-based composite materials-panel products-glued-laminated timber, structural composite lumber, and wood-nonwood composite materials. Review Process: Informally Refereed (Peer-Reviewed).
19. Tsen, S. F., 2013: Determination of structural properties of red seraya plywood using eurocodes compliant testing method. PhD Thesis (online). <http://studentsrepo.um.edu.my/8727/> (Accessed Sep. 20, 2022).
20. Wilczyński, M.; Warmbier, K., 2012: Elastic moduli of veneers in pine and beech plywood. *Drewno*, 188 (188): 47-56.
21. Žiga, A.; Baručija, A.; Čobo, M., 2019: Power regression model: parameters determination. Stepeni model regresije: određivanje koeficijenata modela. Zenica, University of Zenica.
22. Žiga, A.; Begić-Hajdarević, Đ., 2021: Rolling ball sculpture as a mechanical design challenge. In: *New Technologies, Development and Application IV*, pp. 153-161. [https://doi.org/10.1007/978-3-030-75275-0\\_18](https://doi.org/10.1007/978-3-030-75275-0_18)
23. Žiga, A.; Begić-Hajdarević, Đ.; Cogo, Z., 2018: Mechanical toys and souvenirs obtained by co2 laser cutting of plywood. Faculty of Technical Sciences, Novi Sad.
24. Žiga, A.; Cogo, Z.; Kačmarčik, J., 2018: Out-of-plane deflection of J-shaped beam. In: *Proceedings of The 21<sup>th</sup> International Research/Expert Conference, Zenica, TMT-2018*, pp. 269-272.

### Corresponding address:

#### ALMA ŽIGA

University of Zenica, Mechanical Engineering Faculty, Fakultetska 1, 72000 Zenica, BOSNIA AND HERZEGOVINA, e-mail: [aziga@mf.unze.ba](mailto:aziga@mf.unze.ba)